Problem Chosen	2026 MCM/ICM Summary Sheet	Team Control Number
A		2604636

Making Smartphones Smarter

Summary

Sending messages, making phone calls, watching videos, playing games are all things that have been involved in our daily lives. They often produce familiar anomalies, such as rapid drain in the cold, shutdowns under heavy use, or even occasional percentage rebounds. **Smartphone battery drain** appears unpredictable due to coupled factors in battery life, such as time-varying workloads, state-dependent battery characteristics, ambient and operating temperature, and cycle history [1] [2] [3].

In this work, we develop a continuous-time framework based on physics that maps realistic smartphone usage to **State of Charge (SOC)** dynamic and remaining **Time-to-Empty (TTE)**. The battery is represented by an **equivalent circuit model**, while smartphone activities are modeled as power loads, enabling a direct and interpretable link from usage profiles to discharge dynamics.

To keep the model practical and extensible, we build three progressive models. **Model-I** establishes a baseline battery discharge model based on the Thevenin battery circuit with constant open-circuit voltage and internal resistance, and derives SOC and TTE under piecewise-constant task power. This model highlights two fundamental limits that govern runtime: a power feasibility limit with maximum deliverable power and current, and a voltage-cutoff limit, which explains premature shutdown under high load even when SOC remains above zero.

Model-II extends this baseline by allowing key battery parameters, i.e., usable capacity, internal resistance, and open-circuit voltage, to vary with temperature, cycle aging, and SOC. Using public NASA battery data, we reorganize measurements into condition-dependent trends and fit compact low-order functions that preserve expected physical behavior while avoiding overfitting. To prevent premature shutdown, we predict TTE in smartphones and optimize battery life by recommending sequential task execution or low-overlap scheduling These fitted relationships provide an explainable mechanism for why the same workload can draw different current and yield different runtime under different battery states and environments.

Finally, in **Model-III** we use **thermal–electrical coupling** to introduce temperature as a dynamic state variable through a lumped thermal balance equation. The feedback loop is investigated where the discharge current produces ohmic self-heating, temperature changes resistance and usable capacity, and the updated parameters in turn alter current and voltage response. Because of this coupling, Model-III is implemented via single-step numerical iteration rather than a fully closed-form solution, making it suitable for long-duration or high-load scenarios where self-heating is non-negligible.

The model is validated using representative usage profiles. Furthermore, from Apple and Samsung devices across typical modes (Idle, browsing, offline video, and gaming). Sensitivity analyses identify dominant drivers of runtime reduction and quantify the role of temperature and aging. The results are further translated into practical recommendations for end users and operating-system level power-management strategies.

Keywords: Smartphone battery drain, State of Charge (SOC), Time-to-Empty (TTE), Equivalent circuit model, Thermal–electrical coupling

Contents

1 Introduction . . . 1
2 Symbols and Assumption . . . 2
2.1 Symbols . . . 2
2.2 Assumptions . . . 2
3 Models . . . 3
3.1 Model-I Baseline Battery Discharge Model . . . 3
3.1.1 Task-driven Power . . . 4
3.1.2 Nonlinear Current and two Limits . . . 4
3.1.3 State of Charge (SOC) . . . 4
3.1.4 Time-to-Empty (TTE) . . . 5
3.2 Model-II Battery Characteristic Model . . . 5
3.2.1 Data Source and Processing Method . . . 5
3.2.2 Temperature-dependent Characteristics . . . 5
3.2.3 Cycle-dependent Characteristics . . . 6
3.2.4 SOC-dependent Characteristics . . . 7
3.3 Model-III Thermal–Electrical Coupled Model . . . 8
3.3.1 Loop in Model . . . 8
3.3.2 Lumped Model for Heat Balance . . . 9
4 Sensitivity Analysis and Validation . . . 10
4.1 Model-I Task-driven Power Analysis . . . 10
4.1.1 Validation with Experimental data of Constant-Power Scenarios . . . 10
4.1.2 Time-varying Workload Profile . . . 10
4.1.3 Limitation of Model-I . . . 12
4.2 Model-II Battery Parameter Analysis . . . 12
4.2.1 Outputs of Model-II . . . 12
4.2.2 Sensitivity Analysis of Battery Parameters . . . 13
4.2.3 Sensitivity Analysis of Usage Profiles . . . 14
5 Applications . . . 15
5.1 Runtime Prediction for any SOC . . . 15
5.2 Task Optimization for Longer TTE . . . 15
5.3 Ambient Temperature Influence . . . 17
6 Recommendation . . . 18
7 Conclusions . . . 20
7.1 Conclusions . . . 20
7.2 Strength and Weakness . . . 20
7.2.1 Strength . . . 20
7.2.2 Weakness . . . 20
References . . . 21
AI Resource . . . 22

1 Introduction

Smartphones are essential in modern life, but their battery endurance often feels unpredictable. In practice, depletion is driven by the combined effects of workload demand, battery condition, and ambient temperature. These factors interact complexly, and thus the different usage patterns may lead to very different drain rates, and high-power bursts may even cause early shutdown.

We develop a continuous-time, physics-grounded model to describe the dynamics of State of Charge (SOC) and to predict the remaining Time-to-Empty (TTE) under realistic usage scenarios. The battery is represented as an equivalent circuit and phone activities are treated as task-driven power loads, which produce a direct mapping from usage to SOC dynamics.

To keep the framework interpretable and practical, we build three progressive models, as shown in Figure 1.1 Model-I establishes a baseline battery discharge model with idealized battery parameters to investigate workload effects. Model-II introduces battery characteristics varying with SOC, aging, and temperature-related effects. And Model-III integrates temperature through a thermal balance equation, capturing ambient temperature and ohmic self-heating as feedback on resistance and usable capacity.

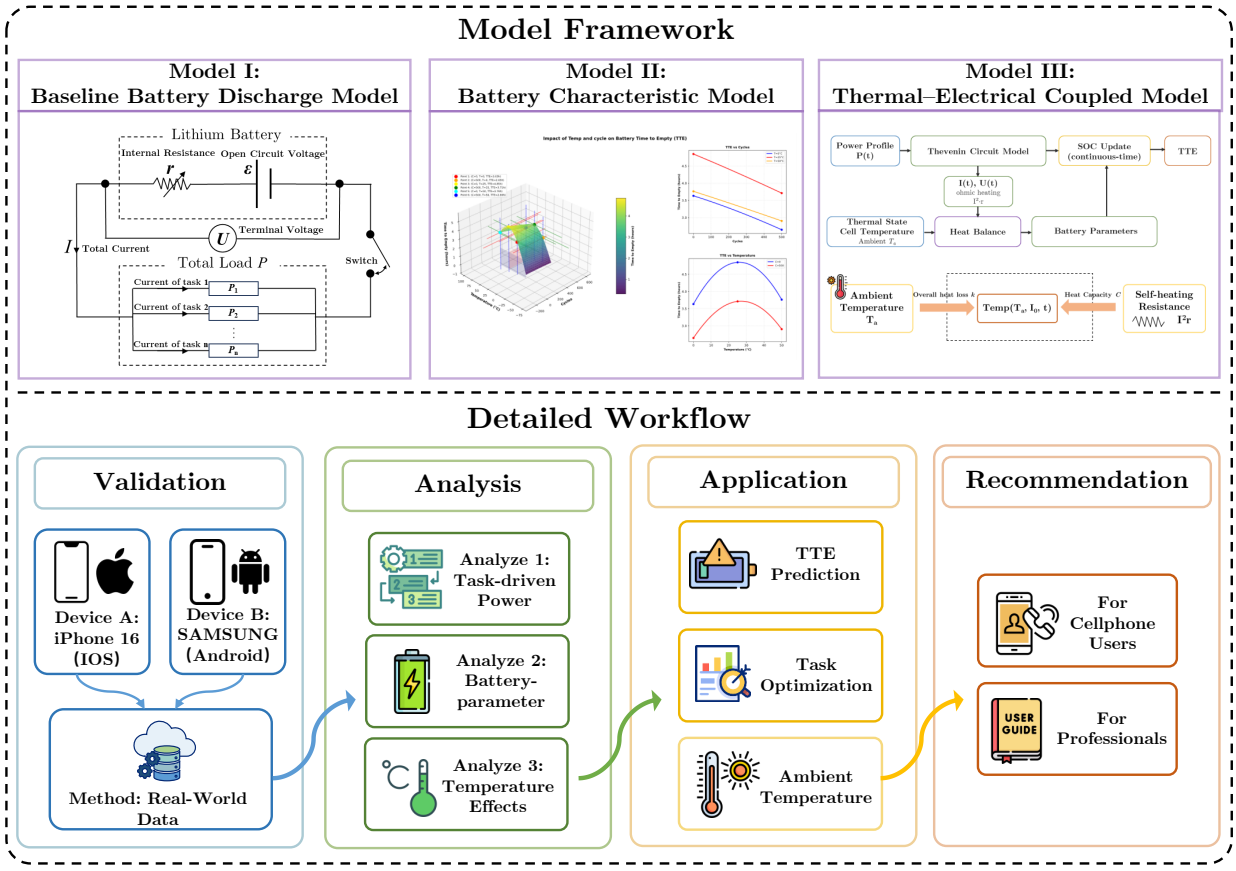


Figure 1.1: Flowchart of our work.

We validate the model using representative experimental results from two devices, i.e., an Apple iPhone and a Samsung Galaxy, under typical scenarios including idle, web browsing, offline video playback, and intensive gaming. In addition, we carry out sensitivity analyses to identify the dominant drivers of runtime reduction. Finally, we translate these findings into actionable recommendations for end users and power management applications.

2 Symbols and Assumption

To keep the model computable and interpretable, we make the following well-justified assumptions. We first state the assumptions shared by all models, and then model-specific assumptions.

2.1 Symbols

The following table summarizes some of the most commonly used symbols in this report.

Table 2.1: Table of Variables.

Symbol	Description	Range	Units
B	Brightness and coloring level	$1 \sim 10$	/
cycle	One loop of charge and discharge	$0 \sim 1000$	/
C	Thermal capacity	36–77	J/K
D	Data rate	$0.1 \sim 1000$	Mbps
$I,\ I_0$	Electrical current, constant current	$10 \sim 2500$	mA
k	Heat Transfer From Battery	0.2	W
P	Total power of all loads	/	W
P_L	Power of screen	$0.5 \sim 1.5$	W
P_{loss}	Power lost by internal resistance	/	W
q	Capacity used	$0 \sim 5$	Ah
$Q_0,\ Q_{\text{nominal}}$	Maximum capacity, effective capacity	$2.4 \sim 5$	Ah
r	Internal resistance	$20 \sim 1000$	mΩ
S	Signal strength	$-50 \sim -25$	dBm
SOC	State of charge	$0 \sim 1$	/
T_a	Ambient temperature	$0 \sim 30$	°C
$Temp$	Average kinetic energy	$-25 \sim 50$	°C
TTE	Time to empty	/	s
$U,\ U_{\min}$	Terminal voltage, minimum voltage	$3.0 \sim 4.5$	V
Greek Symbol			
ε	Open-circuit voltage (OCV)	$3.5 \sim 4.5$	V

2.2 Assumptions

1) **Discharge-only analysis.** We focus strictly on battery discharge under load, but exclude charging phases and "charge-while-use" phases. This keeps the analysis controllable.

2) **SOC definition.** SOC is treated with a consistent reference scale of the nominal full charge. This ensures comparability across scenarios and devices.

3) **Shutdown induced by the voltage cutoff.** A phone shuts down before true empty if the terminal voltage drops below a hardware-required minimum, even when SOC is above zero. This is a common real-world phenomenon under heavy load with internal resistance.

4) **Constant task power.** For each workload mode, the power demand is assumed constant over the duration of that mode, while it may change when the user switches modes. This reduces evaluation complexity while keeping accurate energy accounting for usage patterns.

5) **Dominant power contributors.** We use four dominant contributors, i.e., screen brightness, operating and background activity, processors, and network. This keeps the model analysis

interpretable while preserving the main drivers of battery drain.

6) **Single-cell lithium-ion phone battery.** In Model-I, a single-cell lithium-ion smartphone battery is used for typical phone operation. This constrains the type of battery.
7) **Simplified Thevenin battery circuit [4].** The battery is represented by the simplest Thevenin equivalent, which is an open-circuit source in series with an internal resistance. The simple circuit still captures voltage drop and nonlinearity in discharge behavior.
8) **Parallel equivalent loads.** Concurrent phone tasks are treated as parallel equivalent loads under a common terminal voltage, and total power demand is the aggregate of active tasks. This yields a unified circuit-based representation for multi-task scenarios.
9) **Battery characteristics.** In Model-II, key battery characteristics are allowed to vary with SOC, temperature, and aging level with cycles. These are necessary and dominant characteristics to represent capacity, resistance, and stronger nonlinearity of SOC.
10) **Empirical parameter relationships.** Relationship of battery characteristics are fitted curves from NASA datasets and literature. These relationships are explainable.
11) **Lumped thermal dynamics.** In Model-III, battery temperature is treated as a function over time under ambient temperature and internal heating. This captures the dominant temperature variance for SOC and TTE prediction.

3 Models

3.1 Model-I Baseline Battery Discharge Model

To characterize the power dynamics of a smartphone system, we model the lithium-ion battery using the simplest Thevenin equivalent circuit, see Figure 3.1. The battery is represented by an open-circuit voltage source ε in series with an internal resistance r. As it is a baseline model, ε and r are treated as constants, and thus the impact of workloads can be studied without introducing battery-aging or temperature effects [5].

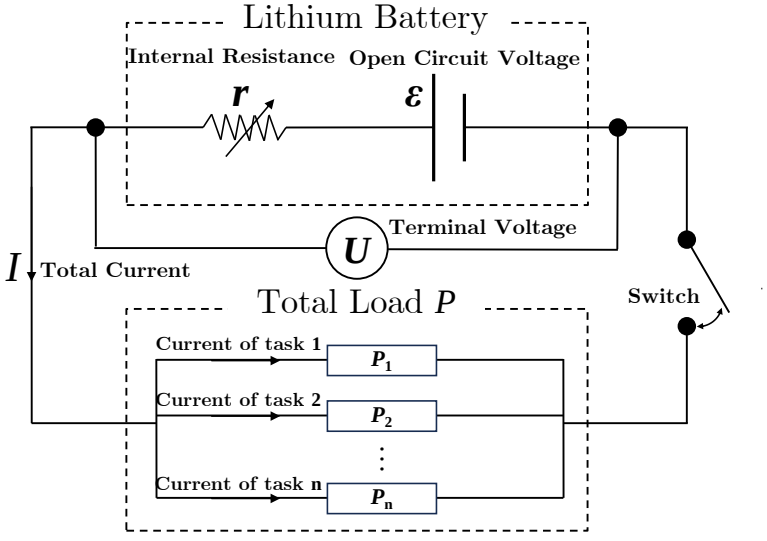


Figure 3.1: Thevenin equivalent circuit of Battery Discharge Model.

3.1.1 Task-driven Power

Loads can be modeled as task-driven power demands. The total power consumption is the aggregate of the powers of n active tasks:

$$P(t) = \sum_{i=1}^{n} P_i(t) \tag{1}$$

These tasks include both software activities and hardware processes, which are represented as parallel equivalent loads sharing the same terminal voltage U. The instantaneous total power changes primarily when the user switches tasks or operating modes. This piecewise-constant representation is practical because real user interaction is inherently stochastic, and a fully continuous closed-form expression for $P(t)$ is neither realistic nor necessary for runtime prediction.

3.1.2 Nonlinear Current and two Limits

Given the Thevenin battery and the external loads, Kirchhoff's law yields a nonlinear relationship that determines the discharge current $I(t)$ under the required power, written as

$$I(t) = \frac{\varepsilon - \sqrt{\varepsilon^2 - 4rP(t)}}{2r} \tag{2}$$

This relationship implies a physical limit: if the demanded power $P(t)$ exceeds the capability of the battery under ε and r, the solution becomes non-physical. Hence, the first limit is $0 \le P(t) \le \frac{\varepsilon^2}{4r}$, or equivalently, the maximum current is $I_{\max} = \frac{\varepsilon}{2r}$.

Furthermore, the terminal voltage satisfies the Thevenin relation $U{=}\varepsilon\text{-}Ir$, which is significantly lower than ε when the current is large under heavy load. However, U must remain above a hardware-defined minimum voltage $U_{\min}$ to keep the electronics operational. This mechanism explains the commonly observed early shutdown under heavy use even if charge remains (SOC > 0). Therefore, the second limit is $U \ge U_{\min}$.

3.1.3 State of Charge (SOC)

The battery state is quantified by the State of Charge, defined on a consistent reference of the initial nominal effective capacity Q_{nominal}.

$$\text{SOC}(t) = \frac{Q_0 - q(t)}{Q_{\text{nominal}}} \quad (\text{SOC} \in [0, 1]) \tag{3}$$

SOC decreases from the initial capacity Q_0 due to the discharged capacity $q(t)$, which is obtained by integrating the discharge current $I(t)$ over time:

$$q(t) = \int_0^t I(\tau)\, d\tau = \int_0^t \frac{\varepsilon - \sqrt{\varepsilon^2 - 4rP(\tau)}}{2r}\, d\tau \tag{4}$$

3.1.4 Time-to-Empty (TTE)

For prediction of runtime, Time-to-Empty (TTE) is defined as the time for SOC to reach the lowest bound or for the terminal voltage to reach the shutdown threshold, whichever occurs first.

$$\mathrm{TTE} = \min\{t_{\mathrm{SOC}},\, t_V\} \tag{5}$$

where t_{SOC} is the depletion time based on SOC, and t_V is the first time the terminal voltage drops below the shutdown threshold $U_{\min}$. When power and consequently current I_0 are approximately constant over a time segment, TTE can be estimated directly as $\mathrm{TTE} = Q_0/I_0$. In general use, however, $P(t)$ and consequently $I(t)$ change across workload modes. We therefore compute t_{SOC} implicitly as:

$$\int_{t_s}^{t_{\mathrm{SOC}}+t_s} I(\tau)\, d\tau = \big(\mathrm{SOC}(t_s) - \mathrm{SOC}_{\min}\big)\, Q_{\mathrm{nominal}} \tag{6}$$

where I may be represented as a piecewise function over time segments, and t_s is the start time point.

3.2 Model-II Battery Characteristic Model

Model-I treats the battery parameters as constants, which is sufficient to study how workload patterns shape SOC and TTE. However, real smartphone batteries are far from this ideal behavior because key parameters change with temperature, usage history (cycle aging), and SOC level. To capture these non-ideal effects while keeping the framework interpretable, we introduce Model-II, where the battery is still represented by the same Thevenin structure, but its fundamental parameters are no longer fixed. Instead, we allow the effective capacity Q_0, internal resistance r, and open-circuit voltage ε to vary with operating conditions.

3.2.1 Data Source and Processing Method

All characteristic relationships in Model-II are extracted from NASA's public lithium-battery dataset [6]. We use this dataset as support for relationships, not as a substitute for the continuous-time model. The raw measurements are reorganized into condition-dependent trends, and each trend is fit with a compact function that (1) matches the data well within the operating range with a simple mathematic function, and (2) remains physically meaningful with smoothness, monotonicity as expected, and reasonable bounds. Although there are lots of experimental data, we treated the data and then kept those variables that significantly affect SOC and TTE behaviors. Those non-sensitive variables were omitted to keep the model minimal. To make the logic clear, we group figures by shared independent variables of temperature, aging cycles, and SOC, which reshape the battery behaviors. In total, Model-II includes six fitted curves in three groups.

3.2.2 Temperature-dependent Characteristics

Figure 3.2 shows that temperature affects the nominal effective capacity and the internal resistance. The usable capacity shows a clear single peak near room temperature (about 25 °C), indicating that both cold and high temperatures reduce the amount of energy the battery can effectively deliver. To capture this trend without overfitting, we fit the capacity–temperature data

using a concave quadratic with its vertex near 25 °C:

$$Q_0(Temp) = -0.000338 \cdot (Temp - 25)^2 + 0.937 \tag{7}$$

In contrast, internal resistance decreases as temperature increases, since higher temperature improves ion transport in the electrolyte and reduces polarization losses. Within the operating range of interest, a second-order polynomial provides a simple and stable approximation, which is

$$r(Temp) = 0.123 \cdot Temp^2 - 10.6 \cdot Temp + 12.4 \tag{8}$$

The two fitted curves explain two important observations in practice, which that is batteries drain faster in cold environments due to reduced usable capacity and increased resistance. The same workload can draw different current under different temperatures.

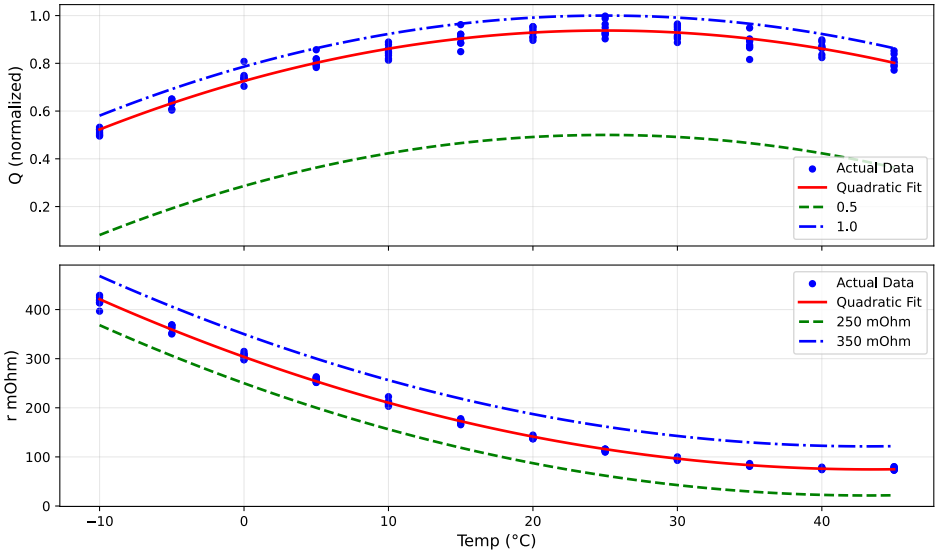


Figure 3.2: Battery characteristic over temperatures.

3.2.3 Cycle-dependent Characteristics

Figure 3.3 shows that cycle aging affects both the nominal effective capacity and the internal resistance. The usable capacity decreases gradually with cycle number, indicating that repeated charge to discharge operation reduces the amount of charge. Over the cycle range supported by the NASA dataset, this downward trend is well captured by a first-order fit:

$$Q_0(cycle) = -0.000415 \cdot cycle + 0.940 \tag{9}$$

In contrast, the internal resistance remains relatively mild at early cycles but increases more rapidly as cycle number grows, reflecting accumulated structural and interfacial degradation that raises the impedance. Within the operating range of interest, a second-order polynomial provides a simple and stable approximation consistent with this accelerating growth:

$$r(cycle) = 0.000982 \cdot cycle^2 + 0.0271 \cdot cycle + 200.4 \tag{10}$$

The two fitted curves explain two important observations: (1) aging reduces runtime primarily through capacity fade, while (2) resistance growth further amplifies voltage drop under load, consequently increase the likelihood of shutdown and make high-power tasks increasingly harmful as the battery ages.

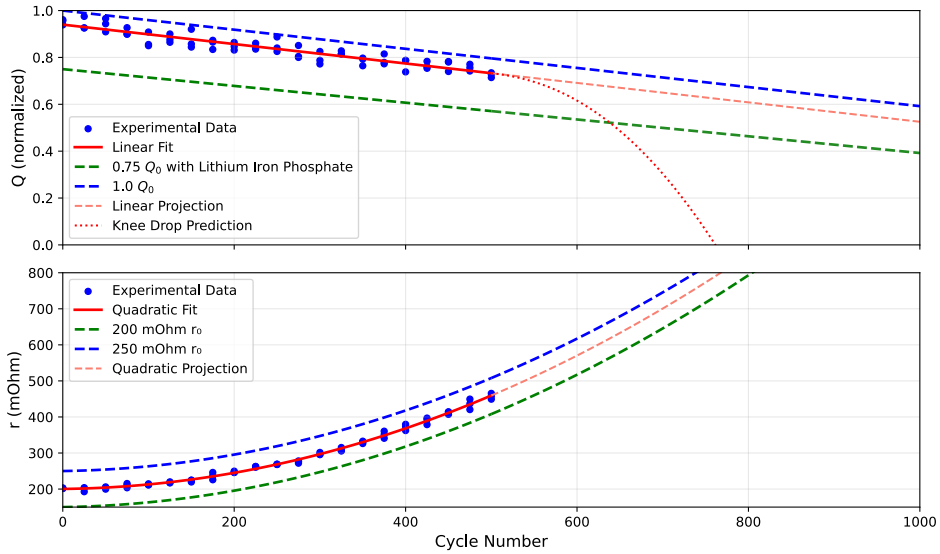


Figure 3.3: Battery characteristic over aging cycles.

3.2.4 SOC-dependent Characteristics

Figure 3.4 shows that the battery's open-circuit voltage and internal resistance varying with SOC. As SOC decreases, the open-circuit voltage drops in a nonlinear manner. This reflects the typical lithium-ion voltage profile. Especially in the mid-SOC range, the voltage changes smoothly, while near the extremes close to full or close to empty the voltage becomes more sensitive. To capture this smooth but nonlinear behavior, the OCV–SOC relation is fitted using a low-order polynomial with sufficient curvature, keeping 3 significant figures:

$$\varepsilon(SOC) = 1.78 \cdot SOC^3 - 2.02 \cdot SOC^2 + 1.20 \cdot SOC + 3.13 \tag{11}$$

This function is simple, continuous, and stable for numerical coupling, while still matching the measured trend across SOC supported by the dataset.

In contrast, internal resistance increases as SOC decreases, indicating that the cell becomes progressively more resistive near the depleted state. Physically, this is consistent with concentration polarization, and when fewer lithium ions are available near the electrode surface, charge transfer becomes harder and impedance rises. Within the operating range of interest, a second-order polynomial provides a compact and reliable approximation with 3 significant figures:

$$r(SOC) = -5.22 \cdot SOC^2 - 22.2 \cdot SOC + 299 \tag{12}$$

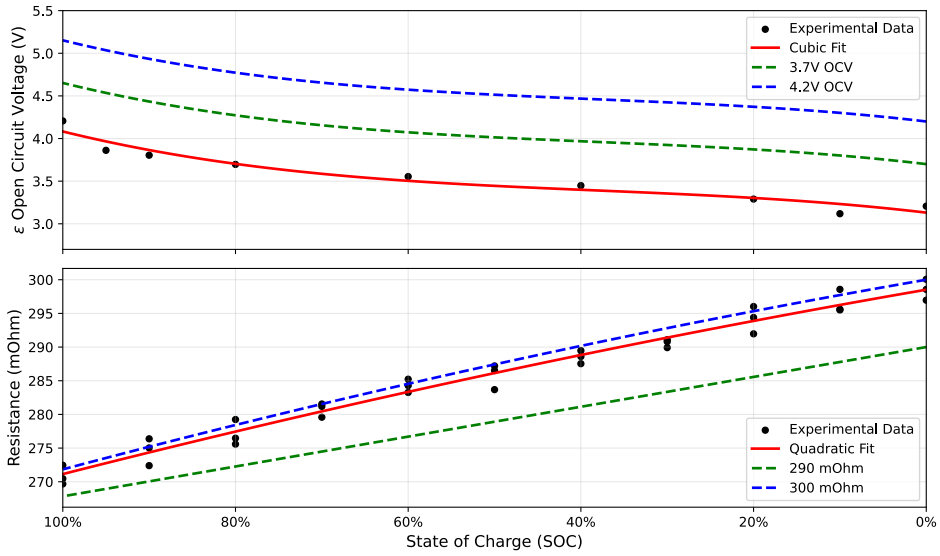


Figure 3.4: Battery characteristic over SOC.

3.3 Model-III Thermal–Electrical Coupled Model

3.3.1 Loop in Model

In practice, battery behavior is strongly temperature-dependent. Ambient conditions change the reaction kinetics and ionic conductivity of batteries, while currents generate internal heat through ohmic loss. These two effects jointly shift the battery's effective capacity and internal resistance, which in turn change the discharge current, voltage drop, and Time-to-Empty (TTE). This coupling process actually creates a loop, as shown in Figure 3.5.

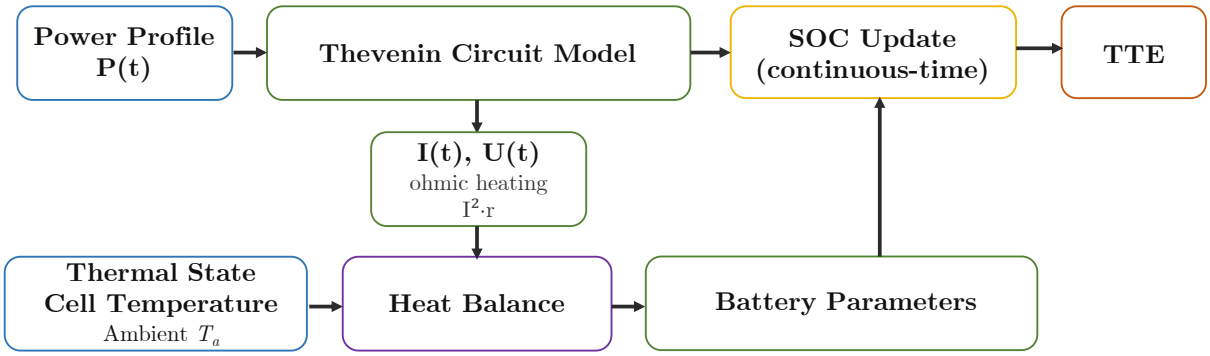


Figure 3.5: Thermal–Electrical loop.

The closed-loop begins from a power profile $P(t)$, which is fed into a Thevenin equivalent circuit to solve the current I and terminal voltage U. The current then updates SOC of battery in continuous time, producing the output TTE. In parallel, ohmic heating I^2r drives a heat balance to change the cell temperature $Temp$, which in turn varies the internal resistance r and effective Q and feeds back to the electrical model. This feedback loop indicates the complex temperature-dependent behavior inside the battery and the environmental temperature.

Model-I and Model-II represent temperature only as a fixed external condition which cannot count for the self-heating and time-varying parameter drift. Therefore, we introduce Model-III to treat temperature as a dynamic state variable.

3.3.2 Lumped Model for Heat Balance

As shown in Figure 3.6, the battery temperature is driven by two sources, the ambient temperature T_a as the baseline thermal environment, and self-heating from internal resistance I^2r during discharge. We represent this with a lumped heat-balance model, where the battery temperature $Temp(t)$ evolves a first-order differential equation. The term I^2r represents the internal heat generation, and the cooling term with k represents heat dissipation to the environment proportional to the temperature difference. The thermal capacity C controls how quickly temperature responds for the heat. This formulation is intentionally minimal yet sufficient: it reproduces both the steady-state temperature rise under sustained current and the exponential approach governed by the thermal time constant.

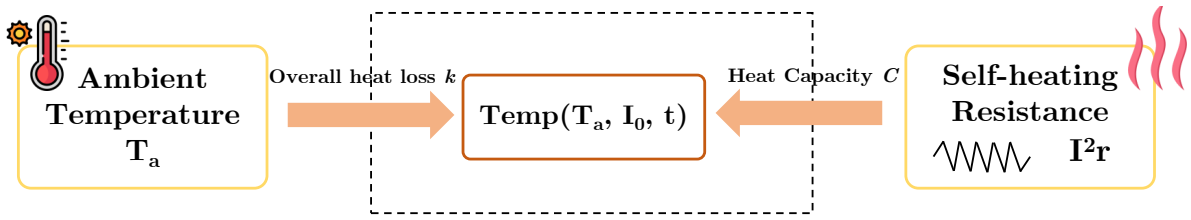


Figure 3.6: Battery characteristic over SOC.

In Model-III, temperature directly feeds back into the battery characteristics introduced in Model II of resistance and usable capacity. As a result, the overall system becomes a coupled model, which can be stated as workload $P(t)$ determines the discharge current $I(t)$; I then produces self-heating and updates $Temp(t)$; the updated $Temp$ modifies battery parameters, such as r and capacity Q; and the modified parameters change the next-step current and voltage response. This closed loop is the key reason Model-III is more complex, yet also more realistic for long-duration or high-load scenarios.

The cell temperature $Temp(t)$ is modeled by a first-order lumped heat balance:

$$C\frac{dTemp}{dt} = I^2r - k\,(Temp - T_a) \tag{13}$$

Here, C is the effective thermal capacity of the battery, which determines how much heat is required for a unit temperature rise. The coefficient k represents the overall heat transfer from the battery to the ambient environment; a larger k corresponds to stronger cooling. T_a is the ambient temperature. The term I^2r presents the resistive self-heating during discharge, while $k(Temp - T_a)$ is the heat to the surroundings, proportional to the temperature difference.

At a steady state, the temperature approaches $Temp = T_a + kI^2r$, showing that sustained higher current leads to a larger temperature rise. Under a constant current I_0, the heat-balance equation admits a closed-form solution:

$$Temp(t) = T_a + \frac{I^2r}{k} + \left[Temp(0) - T_a - \frac{I^2r}{k}\right] e^{-kt/C} \tag{14}$$

The steady temperature rise is caused by self-heating, and the exponential term describes the approach toward steady state with a constant time $\tau = C/k$. This expression makes the thermal behavior explicitly and can be used in the calculation of the Thermal-Electrical Loop.

4 Sensitivity Analysis and Validation

This chapter presents model validation and sensitivity analysis in a progressive manner of our three-level models. First, we validate Model-I as a baseline by comparing TTE predictions against experimental runtime results. Then, Model-II investigates battery characteristics using realistic battery parameters and fitted trends. Sensitivity analysis is realized by perturbing key battery parameters and evaluating changes in TTE and shutdown behavior, allowing to rank the dominant factors that control runtime.

4.1 Model-I Task-driven Power Analysis

4.1.1 Validation with Experimental data of Constant-Power Scenarios

Model-I is a fully analytical circuit-based baseline that evaluates TTE directly from task-driven power inputs. We select two representative flagship smartphones, i.e., iPhone 16 Pro Max (iOS) [7] and Samsung S25 Ultra (Android) [8], to validate the model across platforms, as shown in Table 4.1. The most important parameters for our model are Q_{nominal} and U_{min}.

Table 4.1: Hardware datasheet for smartphones.

Phone	Battery Type[1][2]	Capacity[2]	Screen Type[3]	Voltage[2]	Q_{Nominal}	U_{min}[4]	I_{max}
iPhone 16 Pro Max	S2218	4685mAh	6.9-inch OLED	3.9V	16866C	3.0V	5.5A
Samsung S25 Ultra	EB-BS938ABE	5000mAh	6.9-inch AMOLED	3.9V	18000C	3.0V	6.5A

[1] Data Source from https://www.hubweb.cn/apple-other/battery/
[2] Data Source from https://www.ifixit.com/products/samsung-galaxy-s25-ultra-battery
[3] Data Source from PhoneArena Website
[4] Data Source from Ufinebattery Website

As shown in Table 4.2, four typical scenarios are chosen in analysis, which are Idle, browsing, offline video and gaming. We specify controlled conditions of screen brightness level, network intensity, signal strength, and processor intensity, so that the resulting average power inputs are interpretable and device comparisons remain fair under different scenarios. In addition, the scenario-level total power is the aggregate of the major subsystems, i.e., screen, processor, network, and operating-system background, which is

$$P = P_{\text{background}} + P_{\text{screen}} + P_{\text{processor}} + P_{\text{network}} \tag{15}$$

Table 4.2 provides the total power for each scenario. The TTE calculated from Eq.5. Table 4.2 compares the Model-I calculated TTE with the experimentally reported runtime for two smartphones across four representative scenarios under like conditions [9]. The last two columns report the absolute deviation Δ TTE = (calculated TTE) – (experimental TTE). Overall, the prediction of Model-I is reasonably close to experimental results, and most deviations remain small relative to the total runtime, indicating that the task-power decomposition and the baseline energy–power calculation provide a consistent first-order estimate. Comparing the two phones, we see a significant superiority in performance for iPhone. It could maintain more lifespan even with a smaller battery capacity, showcasing its strength in rendering and system OS compared to Samsung's Android.

4.1.2 Time-varying Workload Profile

Figure 4.1 extends Model-I from single-task constant power to a time-varying workload profile, where each time segment is a combination of concurrent activities (Idle + screen + processor +

Table 4.2: Power assumption of four scenarios for two smartphones and comparison of TTE.

	Tasks	P1: Operation System (W)	P2: Screen (Full brightness) (W)	P3: Processor (Chipset, GPU) (W)	P4: Network (Strong signal) (W)	Total Power (W)	Time-to-Empty TTE Calculated (Hour)	Time-to-Empty TTE* Experimented (Hour)	Delta (TTE) Calculated - Experimented
iPhone 16 Pro Max	Idle	0.05	0.1	0.1	0	0.25	73.08	70.43	2.65
	Browsing by Safari	0.05	0.28	0.42	0.1	0.85	21.5	20.82	0.68
	Video Playback	0.05	0.32	0.13	0	0.5	36.53	33.17	3.36
	Gaming Genshin Impact	0.1	0.75	2.85	0.1	3.8	4.8	4.68	0.12
Samsung S25 Ultra	Idle	0.05	0	0.38	0	0.43	45.35	45.83	-0.48
	Browsing by Chrome	0.05	0.4	0.27	0.08	0.8	24.37	22.18	2.19
	Video Playback	0.05	0.36	0.19	0	0.6	32.5	32.25	0.25
	Gaming Genshin Impact	0.1	1.2	4.02	0.08	5.4	3.6	3.58	0.02

*Data Source from https://www.notebookcheck.net/

network). As a result, the total demand becomes piece-wise function of time, and it can rise sharply when multiple high-load tasks overlap. The specific components of hardware power consumption may also fluctuate because of different brightness, screen quality, and rendering settings. For instance, high power consumption arise when gaming while social media remains active in the background or in split screen. This is precisely why a time-varying profile is more realistic—and also more likely to expose feasibility issues that an average-power model would hide.

To keep the simulation physically meaningful, we enforce the power feasibility limit of the Thevenin battery. Model-I yields a maximum deliverable power $P_{\max} = \dfrac{\varepsilon^2}{4r}$; if any segment satisfies $P(t) > P\,\max$, then the circuit equations have no valid discharge current solution under the assumed ε and r. Therefore, segments exceeding $P\,\max$ (marked with a red box) are flagged as unrealistic operating points, and they motivate the need to (i) constrain workload composition, or (ii) move beyond Model-I by incorporating parameter changes (temperature, aging, SOC dependence) that further reduce the available voltage and power margin.

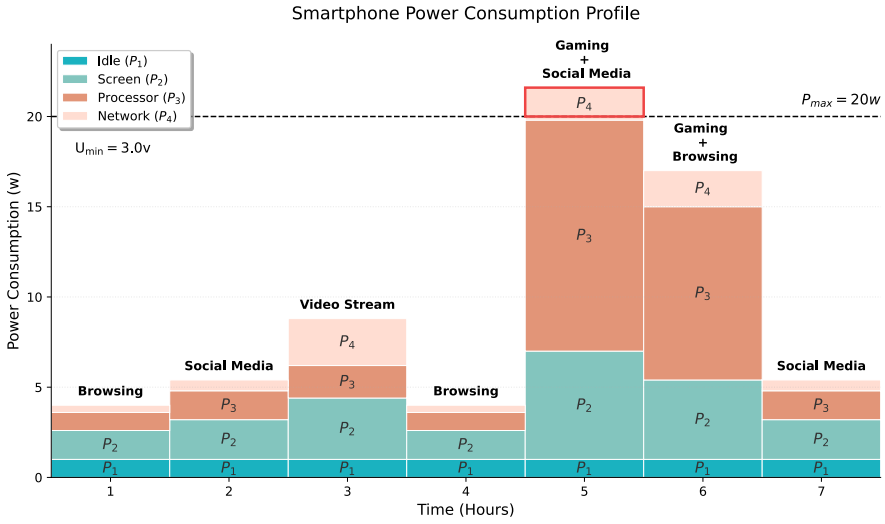


Figure 4.1: Power consumption of time-varying profile.

4.1.3 Limitation of Model-I

Model-I overestimates runtime from experiments. This bias is expected that Model-I assumes fixed battery parameters and a constant effective capacity. In practice, the available capacity and the terminal voltage margin are SOC-dependent, and is reduced by temperature effects and aging. These effects increase effective current demand and can trigger earlier voltage-cutoff shutdown. Since such battery characteristic variations are not included in Model-I, its predictions represent an optimistic upper bound under idealized battery behavior.

In addition, the model cannot directly calculate the terminal voltage (U) because it calculates the current (I) from power (P) and internal resistance (r), but doesn't use this current to update or compute the voltage drop across the internal resistance, which is necessary for determining U.

Therefore, Model-I is best interpreted as a fast algebraic baseline: it is simple to compute, transparent, and suitable for quick comparisons and rough screening of workload impact, but it is not intended to achieve high accuracy under varying environmental conditions or degraded batteries.

4.2 Model-II Battery Parameter Analysis

4.2.1 Outputs of Model-II

Model-II extends the baseline Model-I by introducing battery characteristic parameters, which are the open-circuit voltage, terminal-voltage, internal resistance, and voltage cut-off. These battery characteristic parameters vary with SOC and the operating conditions. Hence, Model-II enables analysis of cutoff terminal voltage $U_{\min}$ and supports local sensitivity tests of battery parameters.

Figure 4.2 involves top and bottom subplots, where the bottom subplot is the piecewise power profile, the same as the variable-load power input in Model-I (Figure 4.1).

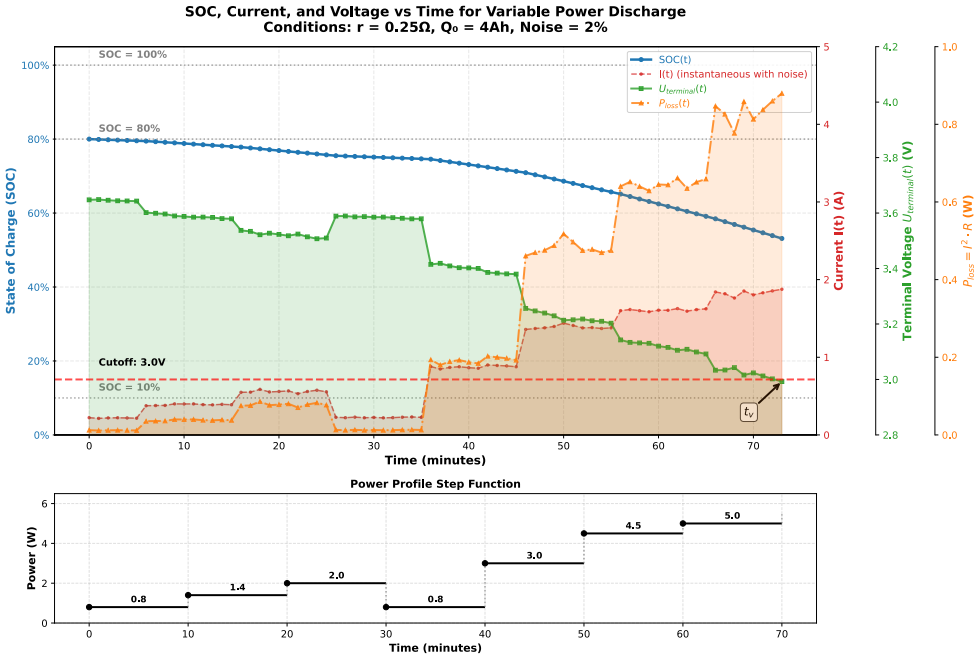


Figure 4.2: Outputs of Model-II with battery parameters.

The top subplot shows several coupled outputs over time, where SOC (blue) decreases continuously in discharge process, and the current I (red) rises when the power steps up and also tends to increase as voltage drops (constant-power discharge requires higher current at lower voltage). The

terminal voltage U (green) declines in discharge and exhibits larger drops under higher loads. And the loss power P_{loss} (orange) increases strongly at higher loads because it roughly related to I^2r.

Crucially, the red dashed horizontal line indicates the cut-off voltage $U_{\min} = 3.0$ V, and the marked t_V point indicates the time when $U(t)$ first reaches the cut-off voltage. This t_V is then the effective TTE, because the device will shut down at t_V even if SOC has not reached its nominal lower bound. The shutdown mechanism presents that TTE is governed by the voltage cut-off event t_V, not only by SOC depletion, which cannot be concluded from Model-I.

4.2.2 Sensitivity Analysis of Battery Parameters

A local parameter sensitivity analysis is applied to the battery parameters of Q, r and $Temp$, and *cycle* (aging indicator). Sensitivity analysis determines which parameters most strongly drive outputs of TTE, terminal voltage, and buttery efficiency. Thus, this parameter is valuable to improvement of TTE.

An analytic derivation may require a closed form solution for the coupled dynamics. However, Model-II involves a nonlinear, strong coupled system under constant-power discharge. Therefore, the solution is implicit and time-varying, and the closed-form expressions for TTE are generally unavailable. As a result, since analytic partial derivatives are not practical, a numerical local sensitivity method is applied instead.

Model-II supports systematic $\pm 10\%$ perturbations about the parameters under investigation. We adopt the iPhone 16 Pro Max as sample. The center parameters Q, r, $Temp$, *cycle*, and the outputs of TTE, U, Efficiency of Battery (defined as effective power over total power) are listed in Table 4.3. Here, sensitivity is defined as how much percentage the output changes when the parameter changes by 10%.

Table 4.3: Sensitivity analysis of battery parameters.

Metric	$Q = 3.3$ (Ah)			$r = 100$ (ohm)			$Temp = 25$ (°C)			*cycle* = 100		
	$0.9Q$	Q	$1.1Q$	$0.9r$	r	$1.1r$	$0.9Temp$	$Temp$	$1.1Temp$	$0.9cycle$	$cycle$	$1.1cycle$
TTE (min)	66.91	74.35	81.78	77.09	74.35	71.6	72.06	74.35	76.67	75.78	74.35	72.93
U (V)	3.715	3.715	3.715	3.734	3.715	3.695	3.705	3.715	3.725	3.72	3.715	3.71
Efficiency of Battery	95.25%	95.25%	95.25%	95.75%	95.25%	94.75%	95%	95.25%	95.5%	95.39%	95.25%	95.13%

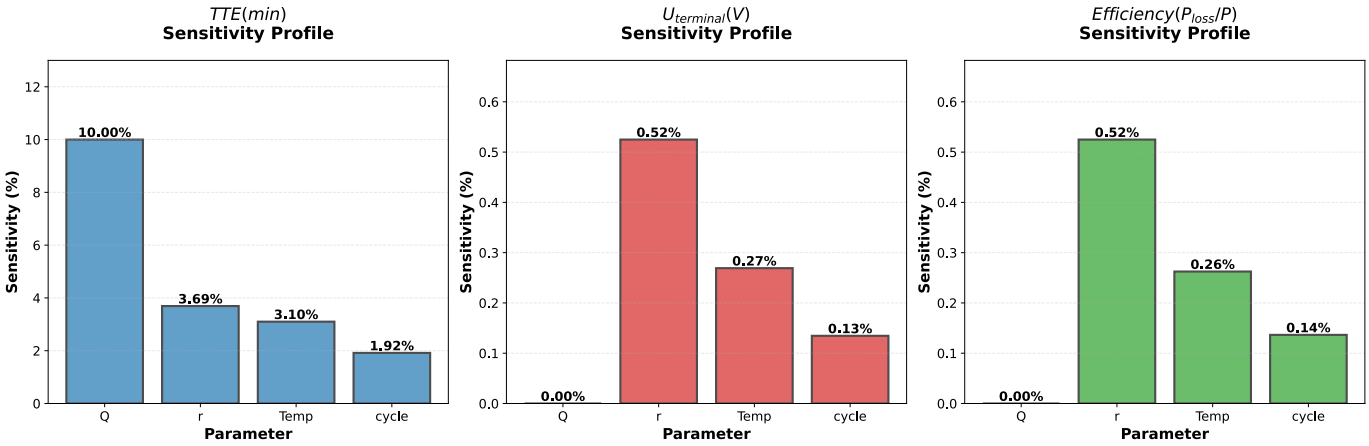


Figure 4.3: Sensitivity profile of TTE, U and Efficiency of Battery.

The results in Table 4.3 and Figure 4.3 are physically consistent. TTE is dominated by capacity $Q \approx 20\%$ sensitivity, because runtime is fundamentally set by the available charge reservoir. The

larger Q directly slows the SOC depletion rate. In contrast, r, $Temp$, and *cycle* affect TTE mainly indirectly by altering voltage and power loss.

Terminal voltage U is most sensitive to internal resistance $r \approx 1\%$ level. Increasing r increases the instantaneous Ir drop under load, reducing the terminal voltage and bringing the system closer to the cut-off threshold. Temperature and *cycle* have weaker effects because they primarily act through parameter shifts, not as direct voltage-drop terms.

Efficiency is strongly controlled by $r \approx 22\%$, with temperature second $\approx 11\%$ and *cycle* third $\approx 6\%$ due to ohmic dissipation.

Overall, Q dominants the runtime, while r governs voltage stability and battery efficiency, temperature and *cycle* act as minor factors. It should be noted that These sensitivity results are local and are only valid in the neighborhood of the chosen analysis parameter set.

4.2.3 Sensitivity Analysis of Usage Profiles

From a usage viewpoint, ambient temperature and aging (cycle count) are treated as external operating factors that shape the effective usage profile. Under these conditions, the model outputs of interest are time-to-empty (TTE), discharge current, and state of charge (SOC).

Figure 4.4 shows the impact of temperature and cycle on TTE. The TTE surface decreases with increasing cycle count, indicating a systematic reduction in usable runtime as battery age. The temperature cross-section exhibits a clear peak near an intermediate temperature around room temperature of 25 degrees, with reduced TTE at both low and high temperatures. This behavior is physically consistent with temperature-dependent performance at low temperature.

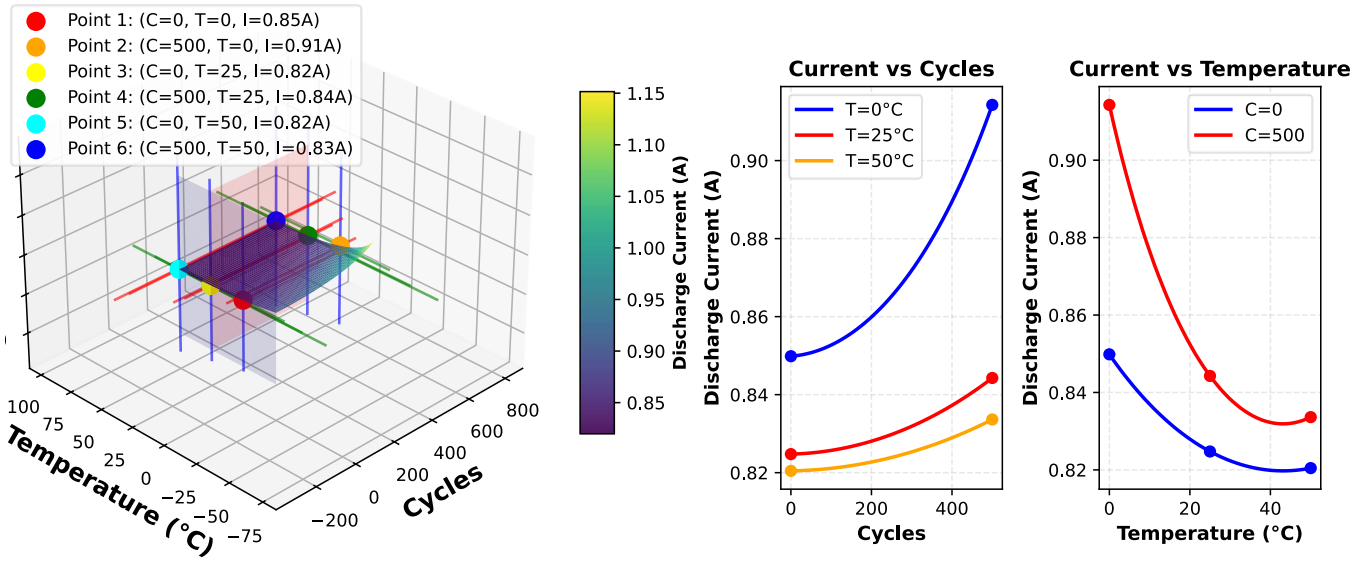


Figure 4.4: Impact of Temp and Cycle on Battery Time to Empty (TTE)

Figure 4.5 demonstrates the impact of temperature and cycle on SOC. SOC decreases with increasing cycle count, indicating reduced effective charge availability and faster depletion under the same operating way. The SOC-temperature curve peaks near moderate temperature and declines toward both low and high temperatures, mirroring the TTE trend and suggesting that usable SOC is maximized under nominal conditions.

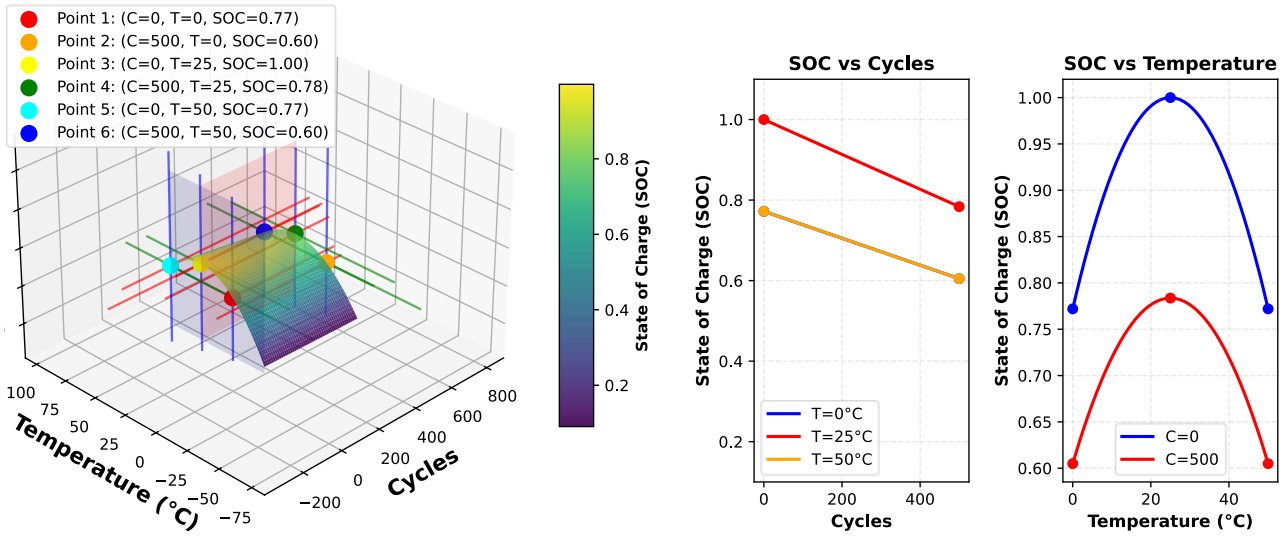


Figure 4.5: Impact of Time and Cycle on Battery State of Charge (SOC)

5 Applications

5.1 Runtime Prediction for any SOC

We present a runtime prediction application based on Model-II. There are two smartphones and four single-task power modes, as described in Section 4.1. Set any initial SOC, we predict time-to-empty (TTE) while accounting for battery parameters and voltage cut-off. This requires instant and interpretable remaining-time estimation with respect to different workload. This function can be applied to real-time smartphone power management and task scheduling.

As shown in Figure 5.1, the results for Apple and Samsung smartphones are reasonable. First, the nearly linear TTE–SOC curves through the origin indicate only single task is carried out, and approximately constant-power discharge with slowly varying parameters of battery. Second, heavier workloads with higher power produce smaller slopes, which means less TTE per unit SOC (see Idle for greatest TTE) because energy is consumed faster. Third, Apple has better performance over Samsung, especially for Idle, but similar values for heavy task of gaming. This can be found in their power requirement for tasks.

5.2 Task Optimization for Longer TTE

The second application of Model-II is to use the model as a decision tool to optimize how multiple user tasks are scheduled in order to save energy. Rather than predicting battery life under a single workload, we consider different task execution plans, e.g., sequential or partially overlapping execution. We use the Apple smartphone as a representative device and select two typical modes with distinct power demands, i.e., browsing with moderate power and gaming with high power.

As shown in Figure 5.2, starting from SOC = 0.5, we execute two fixed tasks: (1) watching video (10 h) and (2) gaming (3.8 h) according to Figure 16.The two task may be Fully parallel (100% overlap), partial parallel (80% overlap), and fully sequential execution (0% overlap). The output is SOC–time curve for each strategy, with the shutdown event explicitly marked when the model predicts a cut-off–limited termination. The results show clear separation among strategies:

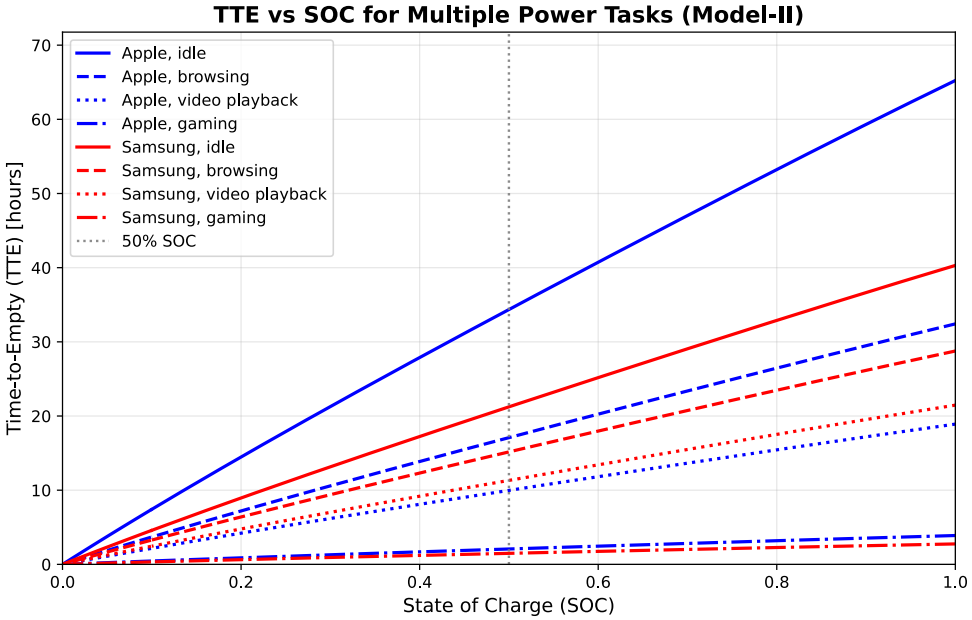


Figure 5.1: Runtime prediction at any SOC.

the parallel case shuts down the earliest, the 80% overlap case lasts longer but still terminates early, while the sequential strategy sustains operation for the longest duration.

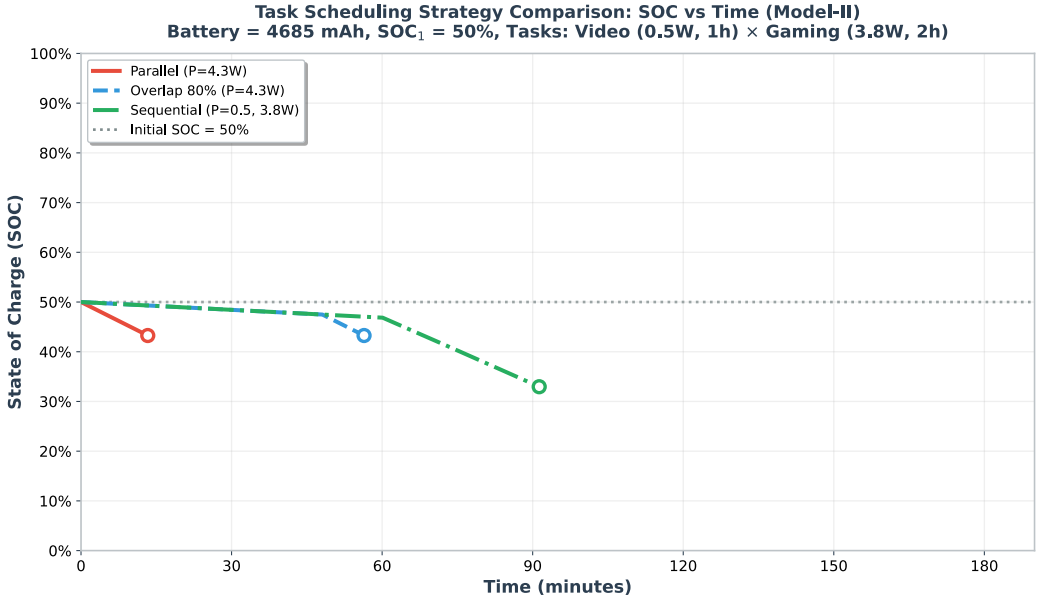


Figure 5.2: Task scheduling strategy.

These outcomes indicate that, under Model-II prediction, the effective runtime is primarily cut-off limited rather than SOC-limited: higher concurrency increases instantaneous power demand, which raises discharge current to trigger an earlier cut-off crossing, even when a substantial SOC remains. For decision-making, the model supports a simple scheduling rule, and avoid high-power overlap and reduce peak power, especially when SOC is moderate or low. Therefore, if the objective is to maximize usable TTE and ensure task completion, a sequential (or low-overlap) schedule is preferred. The overlap should only be used when concurrency is necessary to save time and acceptable at the great cost of reduced runtime.

5.3 Ambient Temperature Influence

This final application employs Model-III (thermo–electrical coupling) to quantify how ambient temperature affects battery life through the battery's internal temperature dynamics. Unlike Model II, ambient temperature T_a is not treated; instead, Model-III updates T_a through a heat-balance model where self-heating and raises battery temperature feeds back to electrical parameters, ultimately shifting the cut-off crossing time and TTE. The engineering value is that it provides a physically grounded way to predict winter battery drain, workload-dependent thermal condition, and temperature runtime, useful for remaining-time estimation, power management policies, and user-facing guidance.

Figure 5.3 shows TTE increasing strongly with ambient temperature and then saturating at warmer conditions. Video playback (0.85 W) is highly temperature-sensitive. It is found that TTE is very low at 20 degrees, rises rapidly toward room temperature, and becomes nearly flat beyond 30 degrees. This is physically consistent. The low temperatures and effective resistance increase, reducing usable energy, so that the terminal voltage reaches the cut-off earlier. In contrast, gaming (3.8 W) exhibits a smaller temperature dependence because the higher current produces stronger self-heating, which partially offset the cold ambient condition by warming by the battery internally.

Practically, the plot implies three clear usage recommendations. In cold environments (especially below 0 degrees, expect substantial runtime loss for light-to-moderate workloads (e.g., video), so keep the phone warm (inside pocket, insulated case) and avoid prolonged exposure to cold air. For high-power tasks of gaming, temperature sensitivity is weaker but battery drain is inherently fast. If instability or sudden shutdown occurs in the cold, reduce load with lower graphic resolution, close background apps, enable power saving and warm the device rather than continuing at peak power. Above 30 degrees, further heating provides little runtime benefit while increasing thermal risk, so avoid direct sunlight and unnecessary heating even if TTE appears saturated.

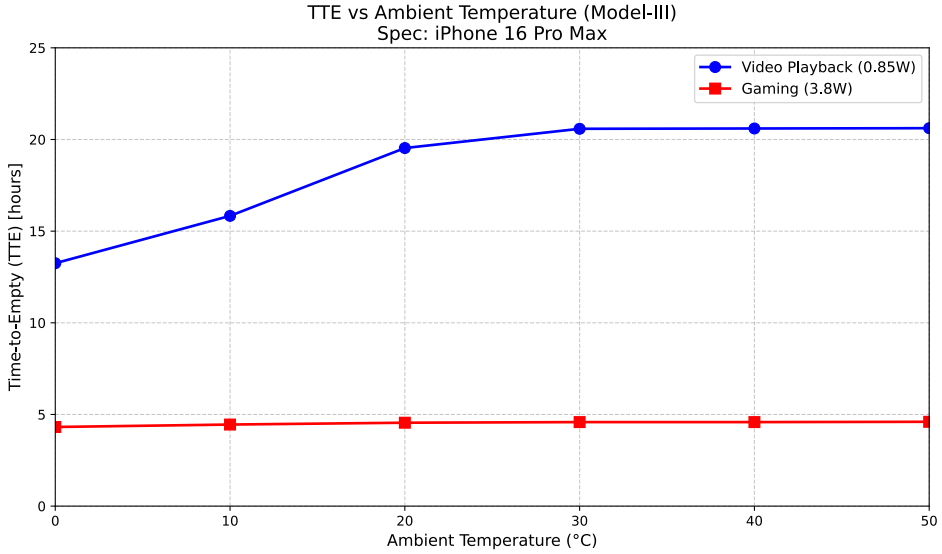


Figure 5.3: Ambient temperature conditions for TTE.

6 Recommendation

We all hate it when our phones suddenly pops out that scary notification saying: "Your phone is below 10% battery." Phone batteries always seem to be insufficient for our needs. However, through some simple tips, you can greatly enhance your phone's battery life.

Battery life is primarily drained by factors like the operating system, screen brightness, processor power, and network usage. Among these, gaming and video playback are the most power-consuming activities, while light browsing and idle time use significantly less power. Typically, the processor accounts for 60-70% of power consumption, with the screen following at around 20%, as shown in Figure 6.1. Additionally, battery capacity can be affected by external conditions such as temperature and cycle history—the number of times the battery is fully discharged and recharged. Over time, these factors can lead to irreversible damage to the battery's health if not managed carefully. By adjusting our user behaviors, we can mitigate these effects and better preserve the battery's lifespan.

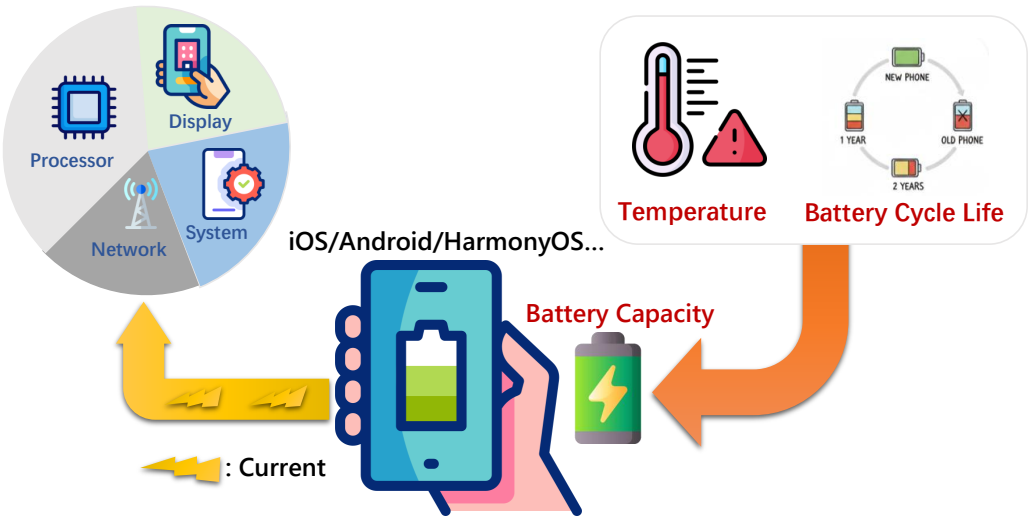


Figure 6.1: Battery Life Factors.

Today's smartphones come with several optimization features designed to manage power consumption, such as low power modes that reduce background activity, limit processor speed, and dim the screen. Many phones also include adaptive battery management that adjusts performance based on usage patterns. Keeping your phone's operating system up to date ensures you benefit from these advances. In our analysis, we identified key differences between iOS and Android. iOS uses a self-restrictive and sufficient strategy for better control, with iPhones demonstrating lower power consumption thanks to powerful A-series chips and Apple's dynamic refresh rate, which reduces the screen refresh rate from 120Hz to 1Hz when Idle. Android, on the other hand, allows users to customize battery usage by controlling app power consumption, restricting background activity, and limiting data access, offering greater control over power management.

Heavy Smartphone Users. For users who consume a lot of power during activities like gaming and video streaming, the screen, processor, and network are all running at full capacity. To save battery, you should optimize performance by lowering game graphics or using battery-saving modes to reduce strain on the processor. Consider downloading videos for offline use, as Wi-Fi consumes up to 50% less power than mobile data. To extend your phone's battery life, avoid

running multiple high-power tasks like gaming or streaming at the same time, and try to use your phone for less demanding activities in between. Finally, lowering the screen brightness, especially in indoor environments, can further conserve battery life. Additionally, avoid using the battery to its limit or to high temperatures, as dropping below the minimum voltage can cause a premature shutdown and potentially lead to irreversible damage.

Business Professionals. If you keep apps running constantly throughout the day, with background tasks like location services, navigation software, and social media syncing, your battery will drain much faster. Regularly close unused apps that don't require constant updates, and enable low-power mode to extend your battery life. Similarly, avoid letting your phone fully discharge, as doing so can cause irreversible damage to the battery's capacity due to chemical reactions in the lithium ions. If you're out and about and need extra "firepower," consider carrying a battery case to avoid running low on energy.

Travelers. When traveling in areas with weak network signals, network power consumption increases because it takes longer to transmit data. Using Airplane Mode or turning off the network in low-signal areas will reduce battery drain. Avoid exposing your phone to extreme temperatures, as both heat and cold can degrade battery life by up to 20-30% in extreme conditions. In cold environments, warm the phone to help current flow, and in hot environments, avoid high-power tasks.

Our model applies to all portable devices. By following these simple yet effective tips, you improve the battery life of both your phone and other devices. Remember, small changes in how you use your phone can make a big difference in how long it lasts on a single charge. Over time, optimizing your phone's battery usage will not only promise benefits to your daily efficiency but also preserve its long-term health.

7 Conclusions

7.1 Conclusions

Our research shows that smartphone battery discharge is a dynamic system influenced by multiple physical variables. Using a continuous-time model based on SOC, we predict Time to Empty (TTE) under different loads. We developed three models: the Baseline Battery Discharge Model, the Battery Characteristic Model (incorporating SOC, cycle history, and temperature), and the Thermal–Electrical Coupled Model, which integrates temperature effects on resistance and capacity.

Validated using data from the iPhone 16 Pro Max and Samsung S25 Ultra, we found that Idle mode offers the longest battery life, while gaming and video watching consume the most energy. During combined tasks, total power can exceed the maximum, and incorporating real-world factors made our TTE predictions more accurate. Our research demonstrates that Model-II can predict TTE accurately, showing that sequential tasks extend battery life by avoiding high-power overlaps.

Our sensitivity analysis revealed that Terminal Voltage (U) has the most significant impact on TTE, while Battery Capacity (Q) shows linear sensitivity. Internal Resistance (r) and Thermal Stress (k) had secondary effects, and temperature and cycle count had minimal impact. The initial voltage remained above the cutoff, ensuring no premature shutdown. All these solutions are deducted from a numerical solution due to the non-linear and coupling nature of our model-III.

These findings lead to actionable recommendations for users and potential strategies for OS-level power management, offering a deeper understanding of smartphone battery depletion and ways to optimize battery life.

7.2 Strength and Weakness

7.2.1 Strength

Our framework employs an equivalent-circuit model that effectively captures real-world phenomena like voltage sag and premature shutdown, accounting for both operating system-level and environmental factors.

By treating software activities as power loads, the model is adaptable to any workload profile, providing a consistent and interpretable link between usage patterns and discharge dynamics.

Our model uses low-order polynomial fitting and provides TTE predictions in real-time with minimal energy overhead. The model can be extended to different types of devices and usage scenarios, making it versatile for use across various smartphone brands and environments.

We use our framework to generate actionable insights for users, such as optimizing power consumption during intensive tasks and making informed decisions about battery health and usage.

7.2.2 Weakness

We assume instant resistance transitions, potentially missing delays during Power spikes.

We used estimations to build our model in 4.1 validation because we could not find the raw data for a specific phone type.

We analyzed only the discharging of a battery, not considering the user's charging of the battery, which also possess great impact on the battery life.

References

[1] M. Singh, J. Trivedi, P. Maan, and J. Goyal, "Smartphone battery state-of-charge (soc) estimation and battery lifetime prediction: State-of-art review," in *2020 10th International Conference on Cloud Computing, Data Science & Engineering (Confluence)*. IEEE, 2020, pp. 94–101.

[2] N. Ding, D. Wagner, X. Chen, A. Pathak, Y. C. Hu, and A. Rice, "Characterizing and modeling the impact of wireless signal strength on smartphone battery drain," *ACM SIGMETRICS Performance Evaluation Review*, vol. 41, no. 1, pp. 29–40, 2013.

[3] H. Li, X. Liu, and Q. Mei, "Predicting smartphone battery life based on comprehensive and real-time usage data," *arXiv preprint arXiv:1801.04069*, 2018.

[4] S. Tarkoma, M. Siekkinen, E. Lagerspetz, and Y. Xiao, *Smartphone Energy Consumption: Modeling and Optimization*. Cambridge University Press, 2014.

[5] G. L. Plett, *Battery Management Systems, Volume I: Battery Modeling*. Boston, MA: Artech House, 2015.

[6] NASA Ames Research Center. (2024) Prognostics center of excellence data set repository. Full repository at Prognostics Center of Excellence. [Online]. Available: https://www.nasa.gov/intelligent-systems-division/discovery-and-systems-health/pcoe/pcoe-data-set-repository/

[7] Apple Support, "iPhone 16 Pro Max - Tech Specs," https://support.apple.com/en-us/121032, 2024, year introduced: 2024. Accessed: 2026-02-02.

[8] "Galaxy S25 Ultra — Features & Highlights — Samsung US — samsung.com," https://www.samsung.com/us/smartphones/galaxy-s25-ultra/, [Accessed 03-02-2026].

[9] D. Schmidt. Apple iPhone 16 Pro Max review - Lots of small improvements for the top smartphone — notebookcheck.net. https://www.notebookcheck.net/{A}pple-i{P}hone-16-{P}ro-{M}ax-review-{L}ots-of-small-improvements-for-the-top-smartphone.900028.0.html. [Accessed 02-02-2026].

AI Resource

1 **Doubao Chat**

Query: What are the benchmarks to measure the smartphone battery drain under different use scenario in industrial in concise wording?

Output: Here are the concise industrial benchmarks for smartphone battery drain across key usage scenarios:

Standby: Idle drain (mA / % per hour, 24h idle test)

Audio Playback: Continuous local/streaming drain, runtime & mW

Video Playback: Fixed brightness looped video, hourly % drain & runtime

Web Browsing: Scripted automated browsing, runtime & per-hour drain

Gaming/3D Load: Sustained 3D benchmark loops, short-period % drop, power draw & throttling

Mixed Daily Use: Weighted composite (call, browse, video, standby), total endurance score

GPS Navigation: Continuous mapping, per-hour % drain

Camera Recording: 4K/1080p video capture, per-minute drain & runtime

Cellular/5G Streaming & Calls: Controlled RF signal, hourly drain vs 4G/5G

Hotspot Tethering: Data throughput-linked drain, % per hour/GB

AOD: Extra standby drain vs AOD disabled (Δ%/h)

Core industrial metrics: discharge current (mA), power (mW/W), energy (mWh), %/hour, total runtime; tested in controlled lab conditions (25°C, fixed brightness/signal, repeated trials).

2 **OpenAI Chat (GPT-5 Thinking)**

Query: Why they all use "Big Buck Bunny" to test the smartphone performance of video playback?

Output: Because Big Buck Bunny is the video world's "default test weight": it's easy to share, easy to reproduce, and stressful enough to reveal real performance differences.

Legal + safe to redistribute: It's released by the Blender Foundation under a Creative Commons license, so companies and researchers can include it in demos, apps, papers, and test packs without negotiating rights. (peach.blender.org)

Everyone can test the same content: Using one common clip makes results comparable across phones, OS versions, and labs. That's why it shows up in established benchmark suites too (not just phone tests). (spec.org)

It's great for "video pipeline" stress: Playback/streaming performance isn't just "CPU speed." It hits hardware decode, GPU rendering, memory bandwidth, thermal throttling, and frame-drop behavior—exactly what many smartphone performance tests care about. Researchers frequently use Big Buck Bunny for these experiments. (NSF Public Access Repository)

Available in lots of standardized encodes: The same clip exists in multiple resolutions/bitrates/codecs (H.264/H.265, etc.), which is perfect for testing 480p vs 1080p vs 4K, or adaptive streaming behavior. (test-videos.co.uk)

Convenient length + repeatability: It's short enough to loop for long runs (battery/thermal tests) while still having motion/detail changes that expose weaknesses. That's one reason it's used in energy and QoE studies. (ACM Digital Library)

If you tell me which "performance test" you're looking at (video playback, streaming, encoding/transcoding, or overall battery drain), I can explain exactly what subsystem Big Buck Bunny is measuring in that context.

3 **Gemini 3**

Query: What means an executive-style summary highlighting main results, insights, and recommendations?

Output: An executive-style summary is a condensed, high-level overview of a larger report or project. It is designed for busy decision-makers who need the core value of a document without reading every page.

Unlike a typical abstract, it is action-oriented and focuses on the "bottom line."

Three Core Pillars

•Main Results (The "What"): These are the concrete outcomes or data points found during the study. Instead of describing the process, you highlight the final numbers, benchmarks, or successful milestones achieved.

•Insights (The "So What"): This explains the significance of the results. It moves beyond raw data to tell the reader what those numbers actually mean for the business, technology, or research field.

•Recommendations (The "What Now"): These are specific, actionable steps based on the findings. This section provides a clear path forward, such as "adopt a specific battery technology" or "increase thermal testing in high-heat environments."

Key Characteristics

•Scannable: Uses bolding, headers, and bullet points so it can be read in under two minutes.

•Independent: A reader should be able to understand the entire situation and make a decision based only on this summary.

•Concise: Usually limited to one page or 5-10% of the total report length.

4 **Claude-Sonnet-4**

Query: Where can I find official performance of the battery for iPhone 16 pro max?

Output: Apple's Official Sources:

Apple's iPhone 16 Pro Max product page - Visit apple.com and navigate to the iPhone 16 Pro Max specifications

Apple Support website - Search for iPhone 16 Pro Max battery specifications

Official tech specs document - Available on Apple's website under the technical specifications section

What you'll typically find:

Video playback time (streaming and downloaded)

Audio playback time

Charging specifications (wired and wireless)

Battery capacity (measured in mAh)

Fast charging capabilities

MagSafe and Qi wireless charging specs

Additional official sources:

Apple Store app - Product details section

iPhone user manual - Available as PDF download from Apple Support

Apple Newsroom - Press releases with detailed specifications

5 **Claude-Sonnet-4**

Query: Where can I find official performance of the battery for Samsung ultra 25?

Output: Samsung's Official Sources:

Samsung's official website - samsung.com, navigate to the Galaxy S25 Ultra product page

Samsung specifications page - Detailed tech specs section

Samsung Newsroom - Press releases and official announcements

Samsung Members app - Product information and specifications

What you'll typically find:

Battery capacity (mAh)

Video playback time

Internet usage time

Talk time

Fast charging speeds (wired and wireless)

Wireless PowerShare capabilities

Charging time specifications

6 **Gemini 3 Fast**

Query: List of all Python matplotlib 3d graph color themes

Output: In Matplotlib, "themes" for 3D graphs are primarily controlled through Colormaps (cmap). These determine how data values (usually the z-axis or a fourth dimension) are mapped to colors on surfaces, scatter plots, or wireframes.

Here is a breakdown of the available color themes categorized by their visual purpose.

1. Perceptually Uniform Sequential

These are the "gold standard" for 3D surfaces. They are designed to be easy to interpret, even for those with color vision deficiency, and they print well in grayscale.

•viridis: The default theme. Transitions from dark purple to yellow.

•plasma: Deep blue to bright yellow/white.

•inferno: Black to bright red/yellow.

•magma: Dark purple to pink/white.

•cividis: Optimized specifically for color blindness.

2. Sequential

Best for showing data that ranges from low to high values.

•Standard Colors: Greys, Purples, Blues, Greens, Oranges, Reds.

•Multi-hue: YlGnBu (Yellow-Green-Blue), BuGn (Blue-Green), GnBu (Green-Blue).

3. Diverging

Use these when your 3D data has a critical middle value (like zero) or a median point you want to highlight.

•coolwarm: Very popular for 3D surfaces; transitions from blue (cold) to red (hot).

•RdBu: Red to Blue.

•seismic: Extreme blue to extreme red with a white center.

•PRGn: Purple to Green.

4. Cyclic

Perfect for 3D plots involving periodic data, like angles or phases, where the start and end values should match.

•twilight

•hsv

5. Qualitative/Miscellaneous

These are less common for smooth surfaces but great for **3D Scatter Plots** where you are categorizing different clusters.

•Qualitative: Paired, Accent, Set1, Set2, Dark2.

•Misc: terrain, ocean, gist_earth (great for topographic 3D maps).

7 **Gemini 3**

Query: What is the normal power consumption of a phone?

Output: In a modern smartphone, normal power consumption is highly dynamic and depends on the specific hardware components in use. Generally, the power draw falls into three distinct categories

Typical Consumption Ranges

Deep Sleep / Standby: 0.01 W - 0.05 W. The phone is on but the screen is off and background tasks are minimal.

Light Use (Reading, Texting): 0.5 W - 1.5 W. This primarily powers the display (at medium brightness) and low-power CPU cores.

Moderate Use (social media, Video Streaming): 1.5 W - 3.0 W. Power increases due to active Wi-Fi/5G radios and hardware video decoders.

Heavy Use (3D Gaming, 4K Recording): 3.0 W - 6.0 W. This is the practical the rmallimit for most phones. Sustaining more than 5 W usually causes the phone to throttle (slow down) to prevent overheating.